



ELSEVIER

Journal of Non-Crystalline Solids 241 (1998) 195–199

 JOURNAL OF
 NON-CRYSTALLINE SOLIDS

Letter to the Editor

Evidence for valence alternation, and a new structural model of amorphous selenium

Xiaodong Zhang, D.A. Drabold *

Department of Physics and Astronomy, Ohio University, Athens, OH 45701, USA

Received 2 June 1998; received in revised form 11 August 1998

Abstract

A molecular-dynamics simulation has been carried out for amorphous selenium. The simulation used 64 atoms in a constant volume simple cubic cell. The pair correlation function, $g(r)$, and structure factor, $S(Q)$, were computed and compared with experimental and previous theoretical studies. The average coordination number is exactly 2. Only one defect, an intimate valence alternation pair type defect was produced. The electronic density of states and the localization of the electronic state also manifest some properties of valence alternation pair defect type. The results give new evidence for valence alternation in a-Se. © 1998 Published by Elsevier Science B.V. All rights reserved.

PACS: 61.43.Dq; 71.23.-k; 71.23.Cq

1. Introduction

The photoconducting and semiconducting properties of amorphous Se [1,2] are connected with the properties and concentration of defects in the structure. In spite of the accumulation of much experimental data, the atomic structure of a-Se remains controversial. Among the numerous studies on a-Se, the models by Street and Mott [3], Kastner et al. [4] have received considerable attention. They postulated that for amorphous selenium defects with the smallest energy were charged pairs consisting of a positively charged triply coordinated atom C_3^+ and a negatively charged singly coordinated atom C_1^- , ‘valence alternation pairs’ (VAP). Here C denotes a chalcogen atom, and subscripts and superscripts represent coordination number and charge state, respectively. Most of the C_3^+ and C_1^- were conjectured to be bound together to form ‘intimate’ VAP (IVAP). This model is successful in explaining the majority of experimental facts and is widely used. There have been many experimental results to support the VAP model [5].

First-principles molecular-dynamics simulation using Car–Parrinello (CP) method [6] by Hohl and Jones [7] suggested that single threefold coordinated atoms C_3^0 are the most numerous defect type. We noticed that the concentration of defects atoms is ~23% in Hohl’s calculation. As to our knowledge, all previous theoretical models have contained well over 10% coordination defects, so that the defects cannot be easily analyzed as isolated entities. Such samples bear only limited relevance to real a-Se, in part because this artificial defect–defect interaction causes a reduction in the local-

gen atom, and subscripts and superscripts represent coordination number and charge state, respectively. Most of the C_3^+ and C_1^- were conjectured to be bound together to form ‘intimate’ VAP (IVAP). This model is successful in explaining the majority of experimental facts and is widely used. There have been many experimental results to support the VAP model [5].

* Corresponding author. Tel.: +1-740 593 1715; fax: +1-740 593 0433; e-mail: drabold@ohiou.edu

ization of the defect wave function. To better connect to experiment, it is necessary to form networks with only a few percent coordination defects and radial distribution function in agreement with experiment. In this paper, we present a network that has geometrical defect densities of a few percent level which is small by the current theoretical standards but is still large compared to experiment. Such a network can give the evidence of VAP in a-Se. The fewer coordination defects can facilitate the interpretation of the total electronic density of states, particularly in the region of the band gap in terms of the coordination defects.

2. Constraints on theory

We used the program of Demkov et al. [8] ‘fireball96’ to construct our network. This model generalizes the non-self-consistent local basis Harris functional local density approximation (LDA) scheme of Sankey and co-workers [9] to an approximate self-consistent form. We tried non-self-consistent (Harris functional) calculation but found that self-consistency was essential to obtain a realistic network. These local basis density functional methods have been successful for several other disordered systems: GeSe₂ [10], a-Si [11], a-GaN [12] and tetrahedral a-C [13].

A cubic supercell of 12.90 Å with 64 atoms placed randomly inside the cube was chosen for the initial configuration of our model. This number gave us a density close to the experimental one of 3.91 g/cm³ corresponding to the liquid Se at ambient pressure and $T=573$ K. After a thermal equilibration at $T=300$ K (a-Se), a steepest descent quench was applied to quench the system to $T=0$ K. All of our calculations were done at constant volume using only the Γ point to sample the Brillouin zone.

3. Results

3.1. Structural properties

The static structure factor of the 64-atom model is shown in Fig. 1 and is in reasonable agreement

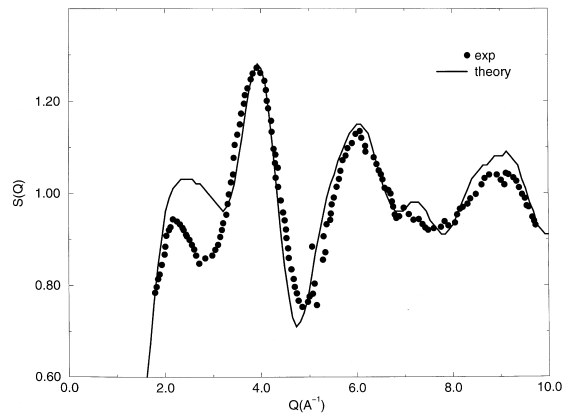


Fig. 1. Comparison of theoretical and experimental (Ref. [10]) static structure factors $S(Q)$ for a-Se.

with the experiment measurements taken from Ref. [14]. The location of all the principal peaks are close to the measured ones. The only important discrepancy is the first diffraction peak. This discrepancy also appeared in the Hohl and Jones' [7] calculation. Generalized Gradient Approximation (GGA) simulations by Kirchoff et al. [15] show better agreement. With an MD cell size of 12.9 Å boundary artifacts will be present for small q .

Fig. 2 shows the computed pair correlation function $g(r)$ and the comparison with the experiment. The experimental data is from Ref. [14]. Prominent peaks at 2.3 and 3.65 Å are evident. A feature is the appearance of the shoulder between

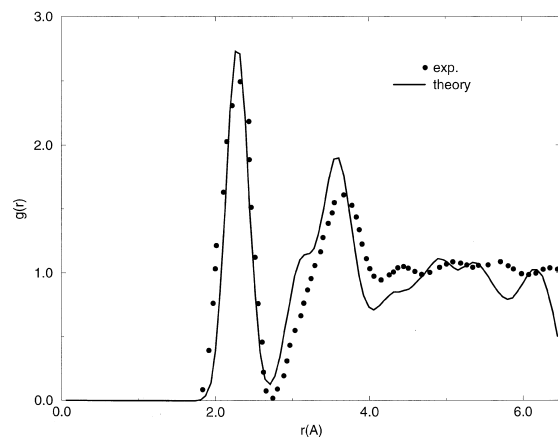


Fig. 2. Pair correlation function $g(r)$ obtained from MD simulation and experiment (Ref. [10]) for amorphous selenium.

first and second peaks. This shoulder also appeared in the Hohl and Jones' calculation [7].

The comparison of computed $g(r)$ and $S(Q)$ functions with experimental data shows that our simulation gives a satisfactory view of local order and distance correlation in a-Se. In Fig. 3 we give an image of our model of a-Se. Only two constituents emerge in our calculations: a large chain with 56 atoms, one of which is a three coordinated defect, connecting with another one coordinated defect, and one six member ring weakly bonded to the chain. We find that the 'distance' between the ring and chain is about 3.05 Å where the shoulder in $g(r)$ appears.

The defect atoms are those atoms whose coordination number differs from two. Here, coordination is defined by the number of neighboring atoms within cutoff, r_c , of the atom, where r_c is taken as the position of the first minimum of pair correlation function, $g(r)$. The defect type is a three-coordinated atom, one of

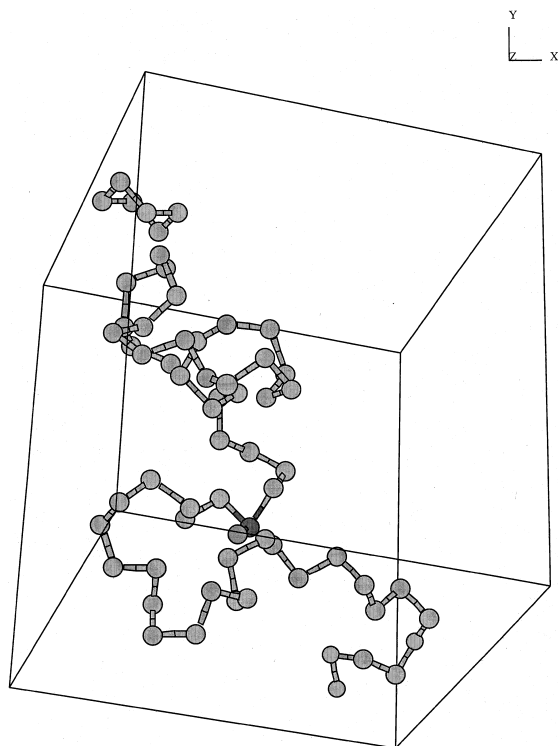


Fig. 3. A unit cell of our model of amorphous selenium. All the bonds are drawn between atoms with separation $d \leq 2.7$ Å.

whose neighbors is a one-coordinated atom (IVAP). This configuration gives an average coordination number of 2. This number also agrees with the diffraction measurements which showed that the atomic coordination number is almost exactly 2 in the low-temperature liquid Se and amorphous Se [14].

3.2. Electronic properties

Fig. 4 shows the electronic density of states (EDOS) and inverse participation ratio (IPR) of our 64-atom model. The inset of the figure is the EDOS and IPR around the gap region. The inverse participation ratio describe the degree of localization. We calculate the 'Mulliken charge', $q(n, E)$, associated with the energy eigenvalue, E , and the atomic site centered at atom number n . For details we refer the reader to Ref. [16]. The IPR(E) is defined as $IPR(E) = \sum_n q(n, E)^2$, where $N=64$ is the number of atoms. Note that $IPR = 1/N$ for completely uniform extended states and $IPR = 1$ for a state completely localized on a single orbital.

The key feature in Fig. 4 is that there are two localized states, one at the top of the valence band and the other at the bottom of conduction band. Very interestingly, the energy difference between the two states is about 2.2 eV which is close to the bandgap of 2.22 eV [1]. This EDOS is in part de-

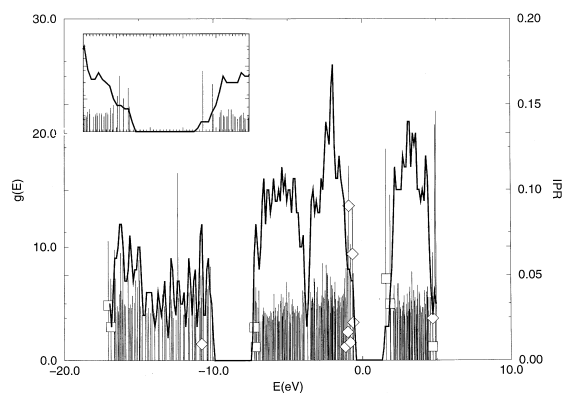


Fig. 4. Electronic density of state and the inverse participation of a-Se. The inset shows EDOS and IPR in band gap region. The diamond stands for $Q_2(n, E)$ for C_1^- atom and the square stands for the $Q_2(n, E)$ for C_3^+ atom. The optical gap contains $E=0$.

terminated by the structure of the a-Se. The diamonds stand for the $Q_2(29, E)$ where atom number 29 is the singly coordinated defect atom and the squares stand for the $Q_2(44, E)$, where atom number 44 is the three coordinated atom. It shows that the localized state at the top of the valence band comes almost from a singly coordinated defect. The localized state at the conduction band edge is localized on the three-fold site and its nearest neighbors, and the singly coordinated defect is more localized. This localization agrees with the early tight-binding calculation by Vanderbilt and Joannopoulos [17]. This characteristic density of state can be interpreted by the chemical bonding configuration of selenium.

Selenium, having 34 electrons, has six electrons outside of closed shells: two 4s and four 4p electrons. For valence energies, a 4s-like band is fairly well separated from three 4p-like bands. Interactions between nearest neighbors split the p orbital into bonding (σ), lone pair (LP) and antibonding (σ^*) bond orbitals. Interactions between different bond orbitals yield bands which give rise to the conduction and valence bands in the solid [17]. For the case of singly coordinated defect sites, at least 3 electrons (3 for neutral defect and 4 for negatively charged defects) are in the LP orbital. The stronger direct π interaction will give rise to localized states above and below the lone pair band edges. If the defect is charged, the defect state above the valence band will be filled. Analogous to that for one coordinated defect, for the three coordinated case, this time there is a pair of σ^* orbitals (and a pair of σ orbitals) which are connected by direct π interaction. The splitting exceeds the band width, and we expect a pair of threefold degenerate localized states [$\pi^*(\sigma^*)$ and $\pi(\sigma^*)$ in our notation] to emerge from the conduction band edges, and similarly for the valence band. In the case of IVAP defect, the one-fold and three-fold defects are neighbors. The defect states associated with the two defect sites remain but are shifted closer to the band edges. In our calculations, the distribution of IVAP defect in the EDOS and IPR nicely fit into above analysis. Our ab initio calculations of EDOS agrees with the descriptions of IVAP defect state by Vanderbilt and Joannopoulos [17] given in their simple tight-binding models.

4. Discussion

4.1. Structure

The main shortcoming of Hohl and Jones's [7] calculations is that the depth of first minimum in $g(r)$ is substantially underestimated. The recent generalized gradient approximation (GGA) calculations [15] give the first minimum in $g(r)$ in much better agreement with experiment, but there is still some discrepancy. So, it is assumed by Kirchoff et al. [15] that GGA is essential to mitigate these problems primarily by getting the proper interatomic distances. We have verified that our Hamiltonian gives a dimer bond length of 2.16 Å which is close to experimental length 2.17 Å. A steepest descent quench was applied to fully relax Hohl and Jones' network to equilibrium with our Hamiltonian [8]. To our surprise, quenching decreases the first minimum of $g(r)$ and the resulting $g(r)$ is in improved agreement with experiment. The static structure factor does not change significantly. Considering the small size of the super cell, the overall agreement with experiment is rather good. Now, we are working on a larger model to reduce the size effect of the supercell. The relaxed Hohl and Jones model only contains six defect atoms. The defect type are $2C_3 + C_1$ (IVAP), C_1 and C_3 . The defect structure results in an average coordination number of 2, a strong signature of dominance of VAP type defect.

Many structural models have been proposed. They often conflict even if apparently supported by more than one experiment. On the basis of X-ray and neutron scattering data, Henninger et al. [18] concluded that a-Se consisted of Se chains in random orientation and 'liquid-like assemblage'. Kaplow et al. [19] were led by their X-ray data to conclude that a-Se is a molecular solid made up of distorted Se_8 molecules. Nevertheless, it is generally agreed that vibration spectra [20] and solution-extraction experiments [19] virtually exclude an atomic ring fraction of more than ~5%. In our MD simulation, it clearly shows that coexistence of long chain and weakly bonded ring is the micropicture of a-Se. The ring fraction in this 64-atom cell is $6/64 \sim 10\%$, a bit large compared to ex-

periment. Another distinct feature in our network is that the ring is six-membered. Because Se_8 and Se_6 rings occur in the monoclinic and the rhombohedral phase respectively, it was long believed that there might be a large concentration of similar rings in a-Se [21]. The Se_8 ring did not appear in our simulation. This is consistent with the result by Kirchoff et al. [15]. Experiment [21] also indicated that a significant Se_8 fraction were shown to be unreliable in a-Se due to equilibration reactions $\text{Se}_\infty \rightleftharpoons \text{Se}_8 \rightleftharpoons \text{Se}_7 \rightleftharpoons \text{Se}_6$.

4.2. Electronic density of states and localization

Since we use self-consistent methods with charge transfer properly accounted for, we are able to distinguish the charge state of the defects in our model. We find that the atoms at the singly coordinated defect site and three-coordinated site have $-0.2e$ and $0.2e$ net charge, respectively. The net charge of the IVAP pair is neutral, in agreement with Kastner et al. [4]. According to the picture of VAP by Kastner et al., the lowest-energy neutral defect is C_3^0 rather than C_1^0 . the VAP and IVAP pair are formed through $2\text{C}_3^0 \rightarrow \text{C}_3^+ + \text{C}_1^-$. So, in the process of forming the a-Se, in addition to the atomic rearrangements accompanying the above configuration changes, there are relaxation effects associated with a change in charge state. We admit that the transfer of $\pm 0.2e$ is small enough that we should not exclude the possibility that the defect is essentially a neutral $\text{C}_3^0\text{-C}_1^0$ pair.

5. Conclusion

The results of static structure factor and pair correlation function are in good agreement with experimental data where available. We provide a mixed long chain and Se_6 ring model of a-Se. The calculation agrees with the prediction that VAP's $\text{C}_3^+ \text{-C}_1^-$ pair is the dominant type in a-Se. We associate the localized states at the top of the valence band and bottom of conduction band to the C_1^- and C_3^+ defects, respectively. The present calcula-

tion gives a strong evidence of valence alternation pairs in amorphous selenium.

Acknowledgements

We would like to thank Dr D. Hohl for providing us with their structural model. We further thank Professor Ron Cappelletti and Dr Ming Yu for helpful discussions. This work was performed in part under the auspices of the US NSF under Grant No. DMR 96-18789 and DMR 96-04921.

References

- [1] J. Mort, *Physics Today* 47 (1994) 32.
- [2] J. Rowlands, S. Kasap, *Phys. Today* 50 (1997) 24.
- [3] R.A. Street, N.F. Mott, *Phys. Rev. Lett.* 35 (1975) 1293.
- [4] M. Kastner, D. Adler, H. Fritzsche, *Phys. Rev. Lett.* 37 (1976) 1504.
- [5] A.V. Kolobov, M. Kondo, H. Oyanagi, R. Durny, A. Matsuda, K. Tanaka, *Phys. Rev. B* 56 (1997) R485.
- [6] R. Car, M. Parrinello, *Phys. Rev. Lett.* 55 (1985) 2471.
- [7] D. Hohl, R.O. Jones, *Phys. Rev. B* 43 (1991) 3856.
- [8] A.A. Demkov, J. Ortega, O.F. Sankey, M. Grumbach, *Phys. Rev.* 52 (1995) 1618.
- [9] Otto F. Sankey, D.J. Niklewski, *Phys. Rev. B* 40 (1989) 3979; Otto F. Sankey, D.A. Drabold, G.B. Adams, *Bull. Am. Phys. Soc.* 36 (1991) 924.
- [10] M. Cobb, D.A. Drabold, *Phys. Rev. B* 56 (1997) 3054; *ibid.* 54 (1996) 12162.
- [11] D.A. Drabold, P.A. Fedders, S. Klemm, O.F. Sankey, *Phys. Rev. Lett.* 67 (1991) 2179.
- [12] P. Stumm, D.A. Drabold, *Phys. Rev. Lett.* 79 (1997) 677.
- [13] P. Stumm, D.A. Drabold, P.A. Fedders, *J. Appl. Phys.* 81 (1997) 1289.
- [14] R. Bellissent, *Nucl. Instr. and Meth.* 199 (1982) 289.
- [15] F. Kirchoff, G. Kresse, M.J. Gillan, *Phys. Rev. B* 57 (1998) 10482.
- [16] Attila Szabo, Neil S. Ostlund, *Modern Quantum Chemistry*, McGraw-Hill, New York, 1989, p. 151.
- [17] D. Vanderbilt, J.D. Joannopoulos, *Phys. Rev. B* 22 (1980) 2927.
- [18] E.H. Henninger, R.C. Buschert, L. Heaton, *J. Chem. Phys.* 46 (1967) 586.
- [19] R. Kaplow, T.A. Rowe, B.L. Averbach, *Phys. Rev.* 168 (1968) 1068.
- [20] G. Lucovsky, in: E. Gerlach, P. Grosse (Eds.), *The Physics of Selenium and Tellurium*, Springer, New York, 1979, p. 178.
- [21] R. Steudel, E.M. Strauss, *Z. Naturforsch. B* 36 (1981) 1085.